



# EFFECT OF DISPERSANTS AND SIZE OF GRAPHITE NANOPLATELETS ON THEIR COMPOSITE PROPERTIES

**In-Hwan Do, Toshiya Kamae, Hiroyuki Fukushima, and Lawrence T. Drzal**  
**Composite Materials & Structures Center, Michigan State University, East Lansing, USA**

**Keywords:** *surfactants, polyelectrolytes, exfoliated graphite nanoplatelets, epoxy, thermal and electrical conductivity*

## Abstract

*Epoxy composites reinforced with single walled carbon nanotube (SWNT), multi-walled carbon nanotube (MWNT), and two different sizes of exfoliated graphite nanoplatelet (xGnP) were fabricated and their flexural properties were compared. xGnP has the potential to replace SWNT and MWNT as reinforcement materials for polymer composites. xGnP/epoxy composites were also prepared in the presence of various surfactants and charged polymers in order to enhance the dispersion of xGnP as well as to improve the compatibility between xGnP and epoxy matrix.. The effect of the addition of the surfactants and charged polymers was evaluated.*

## 1 Introduction

Exfoliated graphite nanoplatelet (xGnP<sup>TM</sup>) is a promising nanostructured carbon which can be used not only as a nanoreinforcing material for polymer composites with excellent mechanical, thermal and electrical properties but also as a support or an electrode material for high efficient energy storage devices [1, 2]. The potential applications of xGnP result from control of its size and modification of its surface chemistry.

The surface of xGnP consists of the basal plane area and the edge area. Excellent dispersion is required for a nanoparticle to be a good reinforcement material. The xGnP surface should have some functional groups compatible with matrix materials, i.e., chemical groups similar to the structure of polymer matrix. Various surface treatment methods can be applied for xGnP surface modification: chemical oxidation in oxidative acids, plasma treatment, and UV/ozone treatment [3~5]. However, such methods are sometimes inconvenient and inconsistent. In addition, they also create only

few percent of oxygen-containing functional groups mostly at the edge area of xGnP, not on the basal plane which is much larger than the edge. Hence, it is of great importance to enhance compatibility with the matrix via the introduction of functional groups on the basal plane area. The choice of dispersants as processing aids in carbon nanostructures-polymer composites is also very important due to their ability to disperse carbon nanostructures in a polymer matrix, preventing the aggregation of carbons which negatively affects mechanical and electrical performance of the composites [6, 7].

In this research, two systems of polymer composites have been prepared. One is epoxy composites reinforced with SWNT, MWNT, and xGnP. The other is xGnP/epoxy composites fabricated in the presence of a variety of surfactants and polyelectrolytes to enhance the dispersion of xGnP and increase an interfacial interaction of xGnP-epoxy at the same time. Mechanical, thermal, electrical, and morphological properties of those composites were measured to evaluate xGnP as a reinforcement material and investigate the effect of xGnP size and the presence of dispersants on the composite properties.

## 2 Experimentals

### 2.1 Materials

Two sets of diglycidyl ether of bisphenol-based epoxy resins/curing agents were applied; one is Epon828/triethylenetetramine (TETA) and the other is Alardite LY1556US/m-phenylenediamine (m-PDA). All of the surfactants and charged polymers shown in Figure 1 and 2 were available from Aldrich and used as received. xGnP with 1 and 15 $\mu$ m in average size denoted as xGnP-1 and xGnP-15, respectively was used as reinforcements. Figure 3 shows typical TEM images of xGnP. The thickness of xGnP is about 10 nm regardless of its size. SWNT

( $d = 1\sim 2\text{nm}$ ,  $l < 50\mu\text{m}$ ) and MWNT ( $d < 8\text{nm}$ ,  $l < 2\mu\text{m}$ ) from Cheap Tubes were also used for comparison purpose.

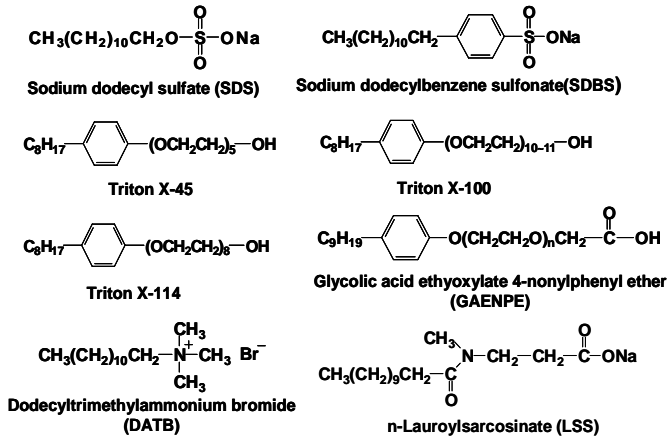


Fig.1. Chemical structures of surfactants used.

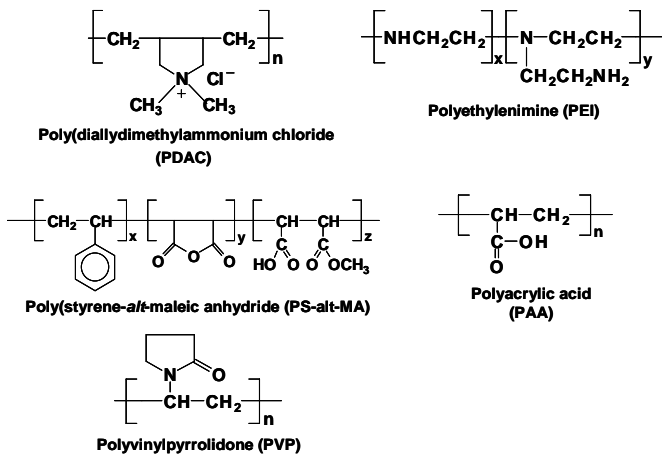


Fig.2. Chemical structures of polyelectrolytes used.

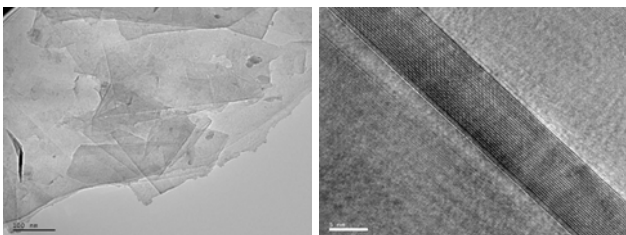


Fig.3. Typical TEM image of xGnP (scale bar: 100 and 5nm)

## 2.2 Sample Preparation and Characterization

For surfactant- and polyelectrolyte-assisted xGnP-15/epoxy composites, 6g of Epon828 was first sonicated with 10mL acetone in which desired amount of surfactants or charged polymers were already dissolved. The amount of xGnP-15

corresponding to 2, 4, and 6wt. % was added. After ultrasonication for another 20min, the mixture was placed in an oven at  $60^\circ\text{C}$  for 2hrs and vacuumed for complete evaporation of the solvent. A curing agent, TETA, was added to the mixture, followed by degassing under vacuum in order to remove air. The degassed suspension was transferred to a silicon mold, followed by curing overnight at room temperature and then postcuring in an oven at  $100^\circ\text{C}$  for 3 hours.

For CNT and xGnP-filled epoxy composites, epoxy resins containing 1wt.% of SWNT, MWNT, or xGnP was processed in the three-roll mill (EXAKT 80E). The speed of the roll was fixed at 250rpm. The mixture was passed through 3, 3, and 5 times at 20, 10,  $5\mu\text{m}$  gap size, respectively. After the three roll mill processing, a curing agent, m-PDA, was added and the other procedures are similar as described above.

The modulus of the composites was measured with Dynamic Mechanical Analysis (DMA) from TA Instruments. Thermal conductivity at low temperature was measured Differential scanning calorimetry (DSC) with at least 5 samples. Electrical conductivity measurements were made after gold electrodes were sputtered on the plasma-treated surfaces on the composites ( $2\text{cm} \times 3\text{cm} \times 0.2\text{cm}$ ) and the two-probe method was used. Morphological properties were investigated with Scanning electron microscope.

## 3 Results and Discussion

### 3.1 Mechanical Properties

The flexural properties of epoxy composites reinforced with MWNT, SWNT, xGnP-1 and xGnP-15 were investigated and their results are shown in Figure 4. While xGnP-1 and MWNT had little effect on the improvement of composite modulus, the best reinforcing effect was obtained from xGnP-15 and SWNT. This suggests the possibility of replacing SWNT and MWNT with xGnP optimized in its size. In addition, xGnP provided the better processability than carbon nanotubes.

In terms of composite strength, only xGnP-1 showed a positive effect but the others resulted in its decrease. This result may come from insufficient mixing cycles because especially in the case of xGnP-15, there were micron-scale agglomerates found at the end of three roll mill process. Based on the observation, longer mixing cycles at 10 and  $5\mu\text{m}$

gap size are required to enhance filler dispersion and reduce filler agglomerates.

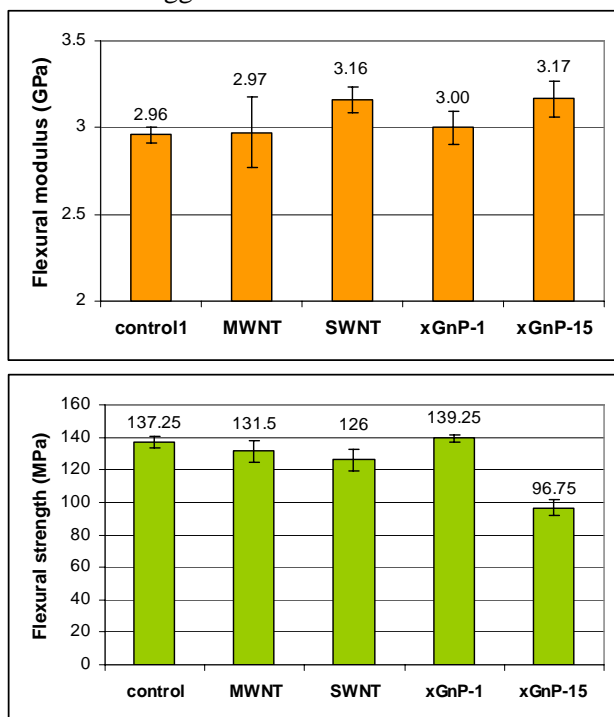


Fig.4. Comparison of flexural modulus (top) and strength (bottom) of epoxy composites reinforced with MWNT, SWNT, xGnP-1, and xGnP-15.

The storage modulus of the composites processed with and without the solvent was investigated. It was confirmed that the effect of a solvent on the mechanical property was negligible in the whole concentration range of xGnP-15, indicating that the solvent was almost completely evaporated and did not cause the degradation of epoxy. The effect of content of dispersants on the composite modulus was also checked, from which the optimal quantity of the dispersant was determined. The highest modulus of the composite was obtained at the presence of 10wt. % of dispersants to xGnP-15 and thus the amount of the dispersant added was fixed at 10wt. % to xGnP-15.

The data of the storage modulus measured for 2wt. % xGnP-15 composites prepared in the presence of various surfactants are plotted in Figure 5. Only 4 surfactants such as Triton X-45, Triton X-114, GAENPE, and SDBS produced an increase of the composite modulus beyond the error margin of unmodified composite. The improvement by Triton X-45, Triton X-114, and GAENPE, and SDBS compared to the other surfactants can be explained in terms of graphite-surfactant interactions, alkyl chain length, and headgroup size [8]. All of them have commonly a benzene ring. The  $\pi$ -like stacking

of the benzene rings onto the basal plane of xGnP-15 contributes to an increase in the binding energy and surface coverage of surfactant molecules to xGnP-15. The different result between Triton X-45 (or Triton X-114, GAENPE) and Triton X-100 arise from the size of headgroup. Although Triton X-100 has a benzene ring, it has larger headgroup than Triton X-45 and Triton X-114. The larger headgroup of Triton X-100 may decrease its packing density on xGnP-15, resulting in less improvement compared to the other Triton series. The different responses of SDBS and Triton X-45 or Triton X-114 arise from different headgroup and chain length. The headgroup of two Triton is polar and larger than that of SDBS; its large size lowers its packing density compared to that of SDBS. The alkyl chain of SDBS is longer than that of the Tritons; its longer alkyl chain increases interaction between xGnP-15 and SDBS by van der Waals attractions. Surfactants with small headgroup in hydrophilic part and a benzene ring and long alkyl chain seem to be preferred according to the results of Triton series and SDBS.

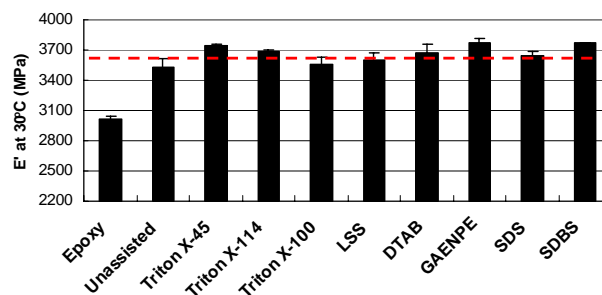


Fig.5. The storage modulus of the xGnP-15/epoxy composites fabricated with various surfactants.

Figure 6 shows the effect of the type of charged polymer on the composite modulus. The substantial increase of the composite modulus was obtained from PS-alt-MA and PAA. The increased modulus of PAA-modified composite may be attributed to the carboxylic groups of PAA which may participate in hydrogen bonding with the epoxy matrix. In the other hand, PS-alt-MA, as shown in Figure 2, has both benzene rings and  $-\text{COOH}$  and  $-\text{COOCH}_3$  in its structure. The former helps to increase the interaction between xGnP-15 and PS-alt-MA through  $\pi$ -like stacking and the latter helps to improve interaction with the epoxy through hydrogen bonding. Hence PS-alt-MA was superior to PAA in improvement of the composite modulus.

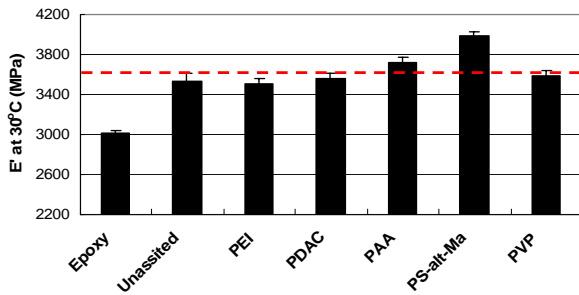


Fig.6. The storage modulus of the xGnP-15/epoxy composites fabricated with polyelectrolytes

SDBS- and PS-alt-MA-assisted composites with different xGnP-15 concentration were fabricated and their storage moduli were compared with that of unmodified xGnP-15/epoxy composite. The result is shown in Figure 7. The composites modified with SDBS and PS-alt-MA showed higher modulus than the unmodified composite in the range of xGnP-15 content investigated. PS-alt-MA has a higher concentration of the benzene ring moiety which enhances interaction between xGnP-15 and dispersant and hydrophilic groups which interact with epoxy than SDBS. This is the reason that PS-alt-MA was more effective than SDBS for the mechanical properties of the composite.

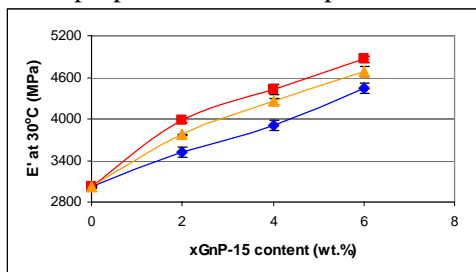


Fig.7. The effect of xGnP-15 concentration of epoxy composites prepared without ((●) and with SDBS (▲) and PS-alt-MA (■).

### 3.2 Morphological Properties

Figure 8 compares SEM images of the xGnP-15 on the fracture surface of control epoxy and the xGnP-15/epoxy composites with and without the addition of the PS-alt-MA which provides the best improvement of the composite modulus among other surfactant and charged polymers. Control epoxy gave a featureless image as in Figure 8a. A low magnification macroscopic view of the fracture surfaces reveals signs of a tougher and stronger material for the composite with the PS-alt-MA than without it, as shown in Figure 8b and 8c. The fracture surface with just xGnP-15 is relatively

smooth, while the fracture surface with xGnP-15 and PS-alt-MA is relatively rough. The difference in the surface roughness explains the different modulus of xGnP-15/epoxy composites fabricated with and without PS-alt-MA. However, significant enhancement of xGnP-15 dispersion in epoxy with the addition of PS-alt-MA could not be quantified.

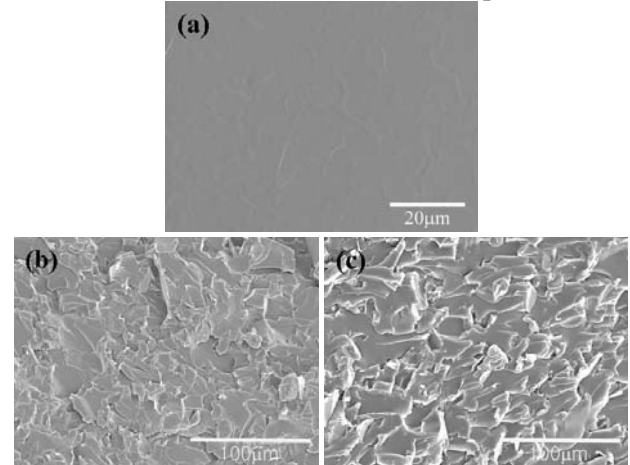


Fig.8. SEM images of (a) control epoxy and xGnP-15 composites fabricated (b) without and (c) with PS-alt-MA.

Figure 9 shows how xGNPs are normally dispersed in epoxy in the presence of PS-alt-MA. Two top pictures in Figure 9 are images of the agglomerated individual xGnP-15, which explain imperfect dispersion even with the addition of a dispersant as well as reveal the further room for the enhanced dispersion of xGnP-15 resulting in further improvement of the composite modulus. Two bottom pictures in Figure 9 show a typical shape and size of xGnP-15 used in this experiment and dispersed individual xGnP-15 separated from the agglomerates of xGnP.

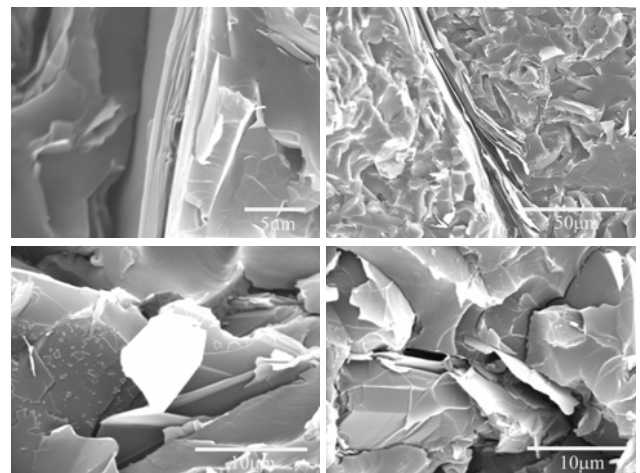


Fig.9. Scanning electron micrographs of xGnP-15 particles dispersed in PS-alt-MA-modified xGnP-15/epoxy composite.

### 3.3 Thermal Properties

DSC measurement is also a useful method for the quick estimation of the thermal conductivity ( $K$ ) of these materials. The slope of the melting curve of a 'standard' metal combined with the sample can be used for the calculation of the thermal conductivity of materials because the slope is proportional to the conductivity of samples [9]. Equation (1) is used to calculate the thermal conductivity of the composites assuming the thickness of samples was kept uniform through DSC measurement.

$$K_x = K_s \cdot \left( \frac{S_x}{S_s} \right) \quad (1)$$

where  $K_x$ ,  $K_s$ ,  $S_x$ , and  $S_s$  represent the thermal conductivity of the sample and reference materials and the slope of melting curve of sample and reference materials. For this experiment, a small amount of Gallium (Ga, mp=29.7°C) of 42.6mg was placed on the surface of the whole samples and handled with a great care in order to keep it from changing its contact area on the sample surface in the middle of DSC measurement. The thickness of samples was kept at 0.5mm ± 0.01. A typical DSC curve obtained for this calculation is shown in Fig. 10. As indicated in the plot, the slope (thick line) for a known Pyrex glass ( $K_s=1.14$ ) [10] is 0.2062 and that (thin line) of epoxy 0.8661.  $K_{x(=epoxy)} = 0.2088$  is obtained by the calculation of eq. (1) from data mentioned above. It is believed that this value for the thermal conductivity of epoxy is reasonable.

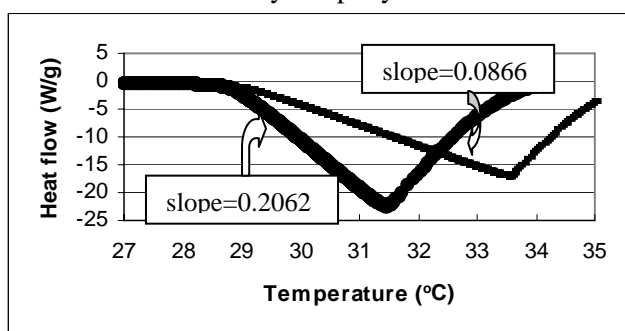


Fig. 10 DSC melting curves of Ga with pyrex glass ( $K=1.14$ ) and epoxy for estimating the thermal conductivity.

The thermal conductivity of the xGnP-15/epoxy composites with and without the addition of PS-alt-MA as a function of xGnP-15 loaded is

shown in Figure 11. Compared to control epoxy, 2 times higher thermal conductivity was achieved with only 2wt. % of xGnP-15 and 4 times higher thermal conductivity with 6wt. % xGnP-15. Even though the thermal conductivity increases with increasing xGnP-15 content for unmodified and PS-alt-MA-modified xGnP-15/epoxy composites, the composites with the addition of PS-alt-MA seemed to show slightly higher thermal conductivity in the composition range due to improved dispersion of xGnP-15 and interaction between xGnP-15 and epoxy.

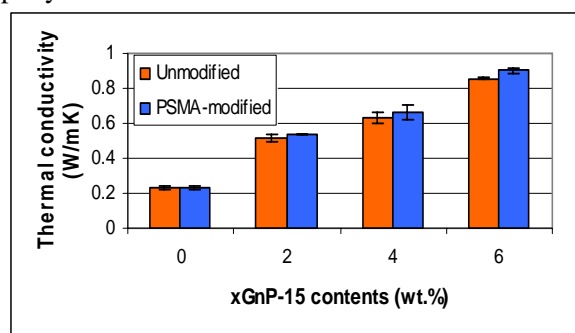


Fig. 11. The comparison of thermal conductivity of xGnP-15 composites in the absence and the presence of PS-alt-MA.

### 3.4 Electrical Properties

The electrical conductivity dependent on the frequency for the xGnP-15/epoxy composites prepared in the absence and the presence of PS-alt-MA are plotted in Fig. 12. Pure epoxy shows a linear decrease of the conductivity in double logarithmic scale as the frequency decreases. This is typical behavior of non-conductive materials in AC impedance measurement. In the case of xGnP-15/epoxy composite prepared without PS-alt-MA as shown in top plot of Figure 12, the electrical conductivity is increasing with increasing xGnP-15 concentration and the conductivity becomes independent of the frequency below 100Hz, which indicates that the composite is relatively low conductive. Similar results were obtained from the composite with the addition of other surfactants and charged polymers except for PS-alt-MA. However, the behavior of the electrical conductivity for the composites fabricated with the addition of PS-alt-MA as in Figure 12 bottom plot shows similar to that of control epoxy. The bulk conductivity of the composite is related to the number of paths through which an electrical current flows. Conduction through the paths may be due to intimate contacts

between conducting particles as well as due to tunneling effect if the distance between the particles is less than a few hundred Å [11]. If individual xGnP-15 were well coated with PS-alt-MA, an electrical current could not flow the path formed by the intimate contact of xGnP-15 coated with PS-alt-MA. The result of the electrical conductivity for the composites with the addition of PS-alt-MA indicates indirectly that each xGnP-15 is well encapsulated by the charged polymer, PS-alt-MA.

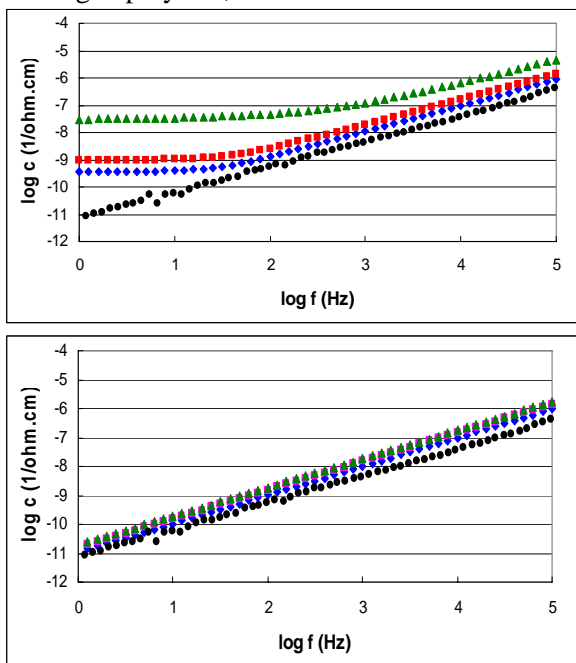


Fig.12. Electrical conductivity of the xGnP-15/epoxy composites (top) without and (bottom) with PS-alt-MA (●: epoxy, ◆: 2wt.%, ■: 4wt.%, ▲: 6wt.% of xGnP-15).

#### 4 Conclusions

xGnP with optimized size seemed to provide reinforcing effect comparable to MWNT and SWNT. Epoxy composites filled with xGnP-15 were prepared in the presence of various surfactants and charged polymers. The substantial increase of the composite modulus was obtained only from the addition of SDBS and PS-alt-MA. Both dispersants have benzene ring favorable for  $\pi$ -like stacking of the molecules on the surface of xGnP-15 as well as small hydrophilic group interacting with epoxy matrix. The thermal conductivity of PS-alt-MA-modified composites showed slightly higher than that of unmodified ones. Interestingly, the PS-alt-MA-modified composites did not show any electrical conductivity in spite of the increased xGnP-15 content.

#### References

- [1] R.K. Agarwal, J.S. Noh and J.A. Schwarz, "Effect of surface acidity of activated carbon on hydrogen storage", *Carbon*, vol. 25, No. 2, p219-226, 1987
- [2] A.K. Shukla, S. Sampath and K. Vijayamohanam, "Electrochemical supercapacitors: Energy storage beyond batteries", *Current Science*, Vol. 79, No. 12, p1656-1661, 2000.
- [3] Liu J, Rinzler AG, Dai H, Hafner JH, Bradley RK, Boul PJ, Lu A, Iverson T, Shelimov K, Huffman CB, Rodriguez-Macias F, Shon YS, Lee TR, Colbert DT, and Smalley RE "Fullerene Pipes", *Science*, vol. 280, p1253-1256, 1998.
- [4] Fukushima H and Drzal L.T, "Graphite Nanocomposites: Structural and Electrical Properties", *Proceedings of ICCM-14*, San Diego, paper 1747, 2003.
- [5] Li J, Kim JK, and Sham ML, "Conductive graphite nanoplatelet/epoxy nanocomposites: effect of exfoliation and UV/ozone treatment of graphite", *Scripta Materialia*, vol. 53, p235-240, 2005.
- [6] Barra S, Demont P, Perez E, Peigney A, Laurent C, and Lacabanne C, "Effect of Palmitic Acid on the Electrical Conductivity of Carbon Nanotubes-Epoxy Resin Composites", *Macromolecule*, Vol. 36, No. 26, p9678-9680, 2003.
- [7] Gong X, Liu J, Baskaran S, Voise RD, and Young JS, "Surfactant-Assisted Processing of Carbon Nanotube/Polymer Composites", *Chemistry of Materials*, Vol. 12, No. 4, p1049-1052, 2000.
- [8] M.F. Islam, E. Rojas, D.M. Bergey, A.T. Johnson, and A.G. Yodth, "High weight fraction surfactant solubilization of single-wall carbon nanotubes in water", *Nano Letters*, 3, p269, 2003.
- [9] Y.P. Khanna, T.J. Taylor, and G. Chomyn, "A new differential scanning calorimetry based approach for the estimation of thermal conductivity of polymer solids and melts", *Polymer Eng. And Sci.*, **28**(16), 1034-1041, 1988.
- [10] G. Hakvoort, L.L. van Reijer, and A.j. Aartsen, "Measurement of the thermal conductivity of solid substances by DSC", *Thermochimica Acta*, **93**, 317-320, 1985.
- [11] H. Kawamoto, in *Carbon Black-Polymer Composites*, Marcel Dekker, New York, 1982, p. 135.